Development of Traction Drive Motors for the Toyota Hybrid System

Munehiro Kamiya*

Toyota Motor Corporation developed in 2005 a new hybrid system for a large SUV. This system included the new development of a high-speed traction drive motor achieving a significant increase in power weight ratio. This paper provides an overview of the hybrid system, discusses the characteristics required of a traction drive motor, and presents the technologies employed in the developed motor.

Keywords: hybrid vehicle, traction drive motor, PM motor, reluctance torque

1. Introduction

In terms of preventing global warming and conserving natural resources, automobiles are playing an increasingly critical role. To reduce the CO_2 produced by automotive vehicles, fuel efficiency must be improved while cleaning exhaust gases as well as ensuring safety.

At Toyota Motor Corporation, solving environmental issues has been being one of our most important tasks, and this focus enabled the company to be successful in making the Prius hybrid in December 1997. In accordance with starting the Prius exports in 2000, the propulsion and combustion characteristics of the THS system were reconsidered from a viewpoint of improving the product performances[(1)]. Further improvements were continued thereafter, so that in April 2003 an increase in motor output by 50% was carried out by boosting up the electrical system voltage and renewing the control system. These innovations all contributed toward producing the next generation, Toyota Hybrid System "THS II", which realized an unprecedented vehicle being coped with both low fuel consumption and a high degree of driving comfort. In that September, Toyota announced this achievement and started sales of the new model Prius featuring THS II[(2)].

In 2005, in order to produce a new hybrid system suitable for a large sports utility vehicle (SUV) with a 3.3 liter engine, Toyota has developed a new class of high speed traction drive motor with more than twice the rotational speed of earlier models, resulting in a significant increase in power weight ratio as shown in Fig. 1.

This paper presents the hybrid system developed in 2005 for SUV, and discusses the technical aspects of the traction drive motor such as the increase in power weight ratio and the reduction of losses.

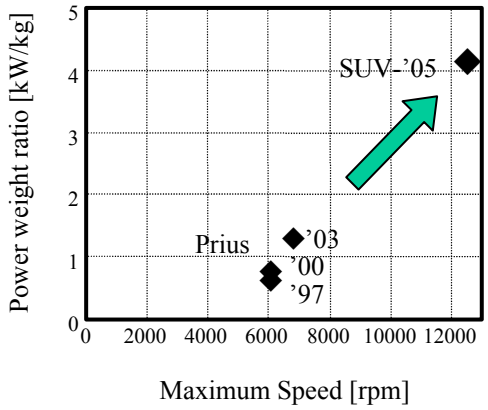

Fig.1. Historical diagram of Power weight ratio improvements in the THS traction drive motor.

2. The Toyota Hybrid System

Fig.2 illustrates the Toyota Hybrid System (THS) which consists of a gasoline engine, THS transmission, inverter, battery, and control units. The THS transmission indicated in the area within the dotted line acts as energy split system in which a traction drive motor, electrical generator and planetary gear are organized. This system makes it possible

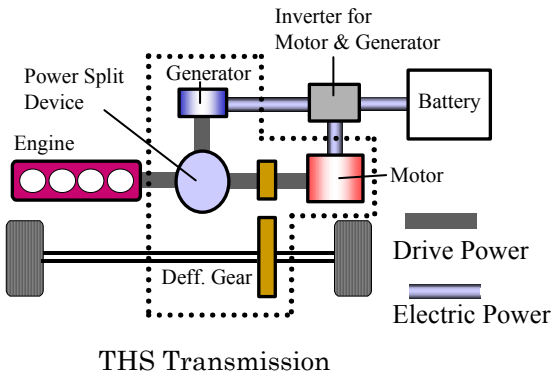

Fig.2. Toyota Hybrid System.

* Toyota Motor Corporation, kamiya@mun.tec.toyota.co.jp
1, Toyota-cho, Toyota, Aichi, 471-8571 JAPAN

to not only deliver whole the engine's power to wheels via differential gear like a parallel hybrid operation, but also convert a part of the engine's power to electric power with the generator and use it to energize the traction drive motor to gain electrical propulsion like a series hybrid operation. As a result, the THS transmission can manage the balance between the engine's power and the motor power for maximum energy efficiency[3] and hence, fuel efficiency can be optimized according to driving status of the vehicles.

Table 1 shows a comparison between the key specifications of the Prius system developed in 1997 and those of the latest system developed in 2005 for SUV. In THS developed up to 2000, DC bus voltage of the inverter and the battery voltage were the same. On the other hand, THS II in the latest Prius in 2003 employed a boost converter, which enabled to adjust the voltage of the battery, motor and generator individually as shown in Fig. 3. This change brought about an increase in motor output utilizing higher supply voltage as well as considerable cost reduction due to decrease in the number of the battery cells.

In the THS II developed in 2005 for SUV, the DC bus voltage was further boosted up from 500V to 650V. At the same time, a reduction device with over twice the reduction ratio was newly adopted as shown in Fig 4, by which the necessary maximum motor torque could be reduced to less than half the required axle torque, allowing the motor down sizing as illustrated in Fig.5. In this way, power weight ratio was significantly improved and a transmission with superior cost performance in terms of size and weight could be realized.

Table 1. THS motor specifications.

System	THS		THS II	
Vehicle	Prius			SUV
E/G	1.5L			3.3L
Launch	1997	2000	2003	2005
DC Bus Voltage	About 274V		500V	650V
Max. Power	30 kW	33 kW	50 kW	123 kW
Max. Torque	305 Nm	350 Nm	400 Nm	333 Nm
Max. Speed	6000 rpm		6700 rpm	12400 rpm

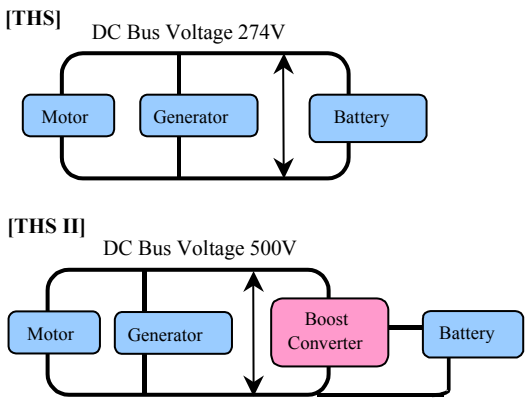

Fig.3. High voltage motors drive system employing a boost DC/DC converter.

3. Required characteristics of the THS traction drive motor

In order to simplify construction, improve transmission efficiency, and achieve smoother acceleration, the THS

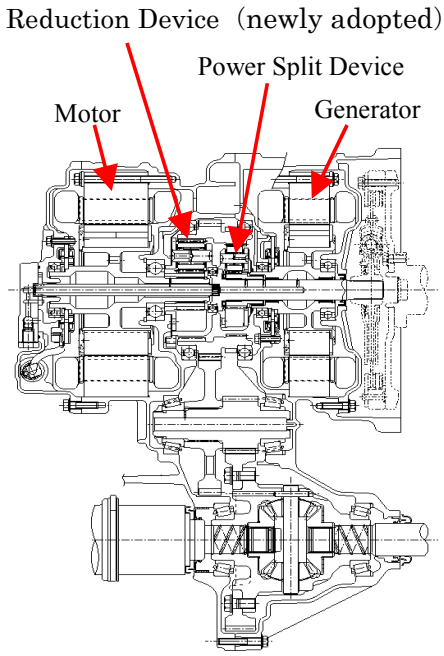

Fig.4. Cross sectional view of THS II.

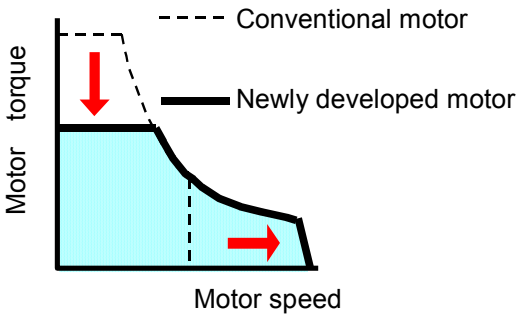

Fig.5. Motor down sizing by reduction gear.

transmission does not have a gearbox, but a single reduction gear. This is because the motor and engine have different torque-speed characteristics so that they can cooperate each other to satisfy total vehicle driving performance. For instance, the motor makes it possible to turn in both forward and reverse directions, take off from a standstill, and obtain the nearly desired torque-speed characteristic for the vehicle through machine design and control. In the case using a single gear system, however, the machine design and control should be considerably difficult because there are so many severe requirements such as high torque capability up to base speed for accelerating and climbing hills and wider operating speed range for achieving sufficient output at the maximum speed.

For the general requirements mentioned above, Interior Permanent Magnet Synchronous Motor (IPMSM) has been selected as the most viable solution for this application because it promises wider torque-speed range under the size and weight restrictions. Besides, the THS traction drive motor must fulfill specific requirements for the vehicle propulsion use as described in following sections.

3-1. Downsizing and weight reduction

As can be seen in Fig.4, the strong point of THS is the reduced size of the unit and its low center of gravity, which are made possible by mounting the traction drive motor, electrical generator, and power distribution mechanism on the same axis as the engine. In this unit, the motor has to be designed so as to be flat shape with larger diameter and shorter axial length in order to realize high torque density and mount on the same shaft

Fig. 6 shows the relationship between the stator outer diameter and the maximum speed of the motors used in existing EVs and HEVs. SUV'05 plotted in the figure, our target motor specification, is located far from the conventional line and therefore, the special design attention to rotor mechanical strength for higher centrifugal force must be paid

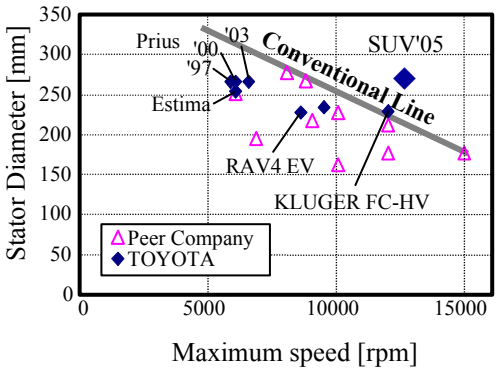

Fig. 6. Relationship between stator outer diameter and maximum speed of recently developed motors for EVs and HEVs.

3-2. Reduction of no-load losses

THS has to provide high power output through the required wide speed range. In spite of that, another important aspect in this application is the fact that the frequent operating points are concentrated at light load region corresponding to Normal City driving. In particular, the motor employed in THS is operated under approximately no-load condition during high speed cruising because the vehicle is running mainly on the engine's power. Fig. 7 illustrates the frequent operating regions during city driving by means of light and shade. The no-load loss reduction in these frequent operating regions is necessary for improving actual fuel efficiency. Fig.8 shows major motor losses distribution for whole operating range. As shown in Fig. 8, iron loss accounts for the majority of motor losses under the most of frequent operating regions. Hence, iron loss reduction is an indispensable task in the system developed in 2005.

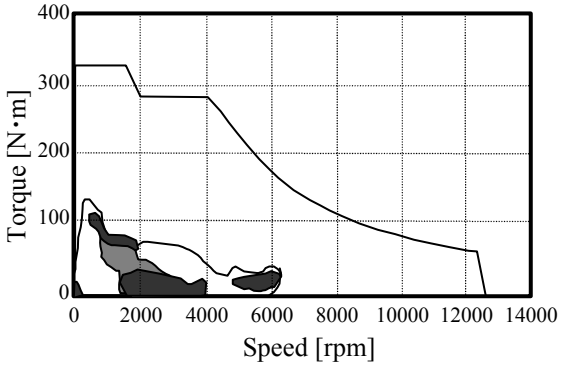

Fig. 7. Frequent operating regions in city driving.

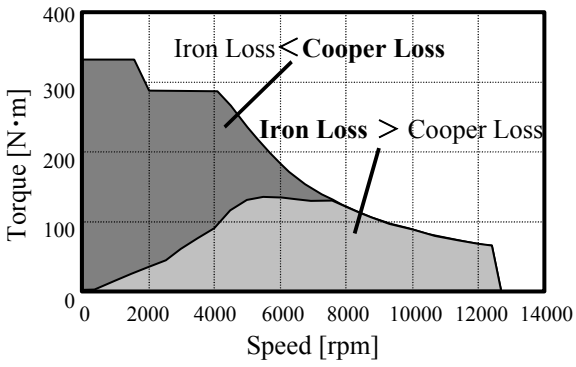

Fig. 8. Major motor losses distribution.

3-3. Limits of no-load induced voltage by efficient utilization of reluctance torque

Given that harmonics in air-gap flux distribution can be neglected, torque and voltage equations of IPMSM on the *d-q* coordinate can be expressed by Eqs. (1) and (2), respectively. Where, T is torque, P_n is the number of poles, φ_m is the armature flux linkage due to the permanent magnet, i_d and i_q are the *d*- and *q*-axis current, respectively. L_d and L_q are the *d*- and *q*-axis inductance v_d and v_q are voltage on the d-q coordinate, R_a is the electrical resistance per phase, ω is electrical angular velocity.

$$T = P_n \varphi_m i_q + P_n \left(L_d - L_q \right) \; i_d i_q \qquad (1)$$

$$\begin{pmatrix} v_d \\ v_q \end{pmatrix} = \begin{pmatrix} R_a & -\omega L_q \\ \omega L_d & R_a \end{pmatrix} \begin{pmatrix} i_d \\ i_q \end{pmatrix} + \begin{pmatrix} 0 \\ \omega \varphi_m \end{pmatrix} \qquad (2)$$

The second term in Eq. (2) corresponds to the voltage induced by the fixed permanent magnet field, which always occurs as long as the motor is rotating. As vehicle speed increases ω also increases, field weakening control is generally applied to the motor in order to limit the induced voltage less than inverter dc-bus voltage. However, when some control failures are happen during the high speed cruising, the filed weakening current id should be uncontrollable so that the higher voltage than the dc-bus voltage could be induced on the motor terminal. Even so, since the primary circuit must be protected, the value of φ_m has to be designed considering the maximum voltage rating of switching devices used in the primary circuit and the presumed maximum speed ω. If φ_m is restricted the permanent magnet torque represented by the first term in Eq.(1) Is restricted as well, and so in order to ensure necessary torque the reluctance torque given in the second term in Eq.(1) must be utilized effectively. Moreover, since an increase in the permanent magnet torque results in an increase in iron loss under the light-load and intensive field weakening operations, a motor design that makes the best use of the reluctance torque is also important from a standpoint of no-load loss reduction.

In addition to the application-oriented design aspects mentioned above, there are many requirements such as noise and vibration; quietness is one of the key selling points of electric vehicles, and torque ripple which causes slight vibrations at vehicle starting must be minimized. Furthermore, mass production of these vehicles demands high reliability and low cost. Accordingly, this development has to be accomplished with well-balanced as well as in high quality for these requirements.

4. Design and development of the traction drive motor

Restating the requirements that have to be fulfilled by traction drive motors, the major points of consideration are:

1) Rotor mechanical strength reinforcement
2) Iron loss reduction
3) Effective use of reluctance torque

Generally speaking, it is desirable to select a large number of poles, taking the increased rotor mechanical strength and the magnet volume minimization into account, but iron loss could be a problem in the target high-speed traction motor drive. Hence, in this design and development stage, 8-pole rotor configuration has been selected from the viewpoints of iron loss reduction and compatibility with previous systems, and considered as a point of departure in following subsections.

4-1. Embedded permanent magnet placement

According to the second term in Eq.(1), to design the IPMSM which makes the most of reluctance torque is to maximize the inductance difference L_q–L_d. From a magnetic design view, it can be achieved by maximizing the permeance along the *q*-axis while keeping the minimal d-axis permeance, i.e., the minimal d-axis inductance being accordance with the desired field weakening capability. As one of feasible designs in order to maximize the *q*-axis permeance, it is well-known that flux barriers are placed along the vector potential contour lines which can be obtained from FE analysis using entirely iron rotor under only the excitation with q-axis current[4],[5]. In this case, permanent magnets are embedded in the flux barriers. Besides, although a rotor construction with multi-flux barriers has been proposed[6], the constructions with more than two layers flux-barrier seem to be impractical for mass production in terms of cost and manufacturability because thin permanent magnets have to be embedded. For this reason, a single flux-barrier is treated in this design and development.

On the assumption that permanent magnets are placed along the vector potential contour lines, magnet opening angle θ as shown in Fig. 9 must be decided. Usually, θ should be as large as possible for increasing the magnet torque. However, on the contrary a smaller θ is more desirable to reduce the iron loss and the no-load back-emf. Thus, there exists an optimum value for θ. In this design, θ is determined so as to minimize Total Harmonic Distortion (THD) of the air gap flux density distribution as an alterna-

tive index of the iron loss reduction.

Fig. 10 shows the magnet embedding layouts and each corresponding air gap flux density distribution each rotor model uses the same amount of magnet. Type A and B have a flat shape magnet but with the different embedded depths. In Type C, the embedded magnet is arranged in a V-shape. The corresponding air gap flux density distributions calculated from FEM analysis differs in amplitude depending on the magnet embedding layout. However, their distribution widths are almost the same, so that they can be regarded as a rectangular distribution with the width θ. In this case, THD of the air-gap flux density distribution can be expressed with the following equation as a function of θ.

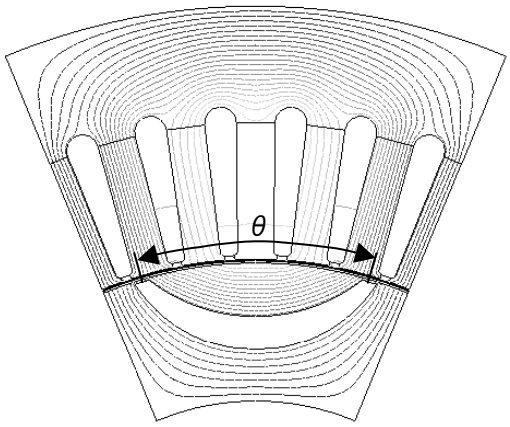

Fig. 9. Vector potential contour lines and θ.

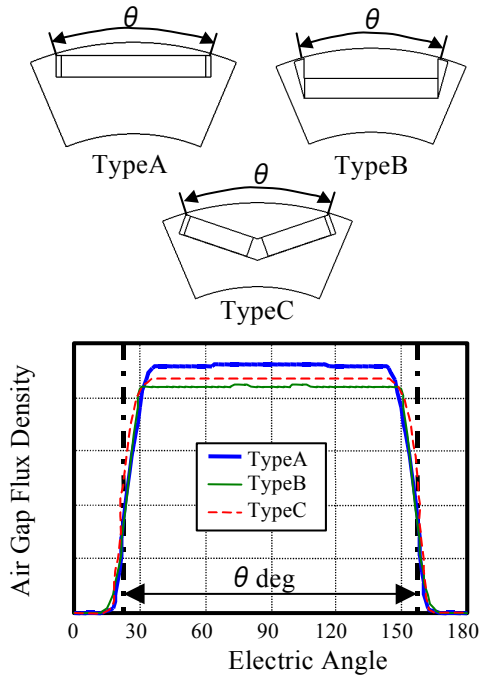

Fig. 10. Air gap magnet flux distribution.

$$\mathrm{THD} = \sqrt{\frac{\pi\theta}{8} - \sin^2\frac{\theta}{2}} \Big/ \sin\frac{\theta}{2} \qquad (3)$$

The optimum distribution width θ_{opt} that minimizes the THD in Eq.(3) can be found θ_{opt} = 133.5 deg. From a standpoint of iron loss reduction, accordingly, the $\theta_{opt}$is treated as the reference value in following consideration.

4-2. Bridge design considerations

In IPMSM, the bridge that supports the flux barrier segment is necessary to ensure the rotor mechanical strength. However since the flux leakage of the permanent magnet increases due to the existence of the bridge, it is desirable to design the bridge width and number as small as possible within the range acceptable for the rotor strength. The optimum bridge design is examined here taking into the restrictions on reluctance torque and magnet opening angle account.

In order to analyze the stress on the bridge by centrifugal force more effectively, a simple FE model is introduced in which the bridge area only employs beam elements. The beam model has an ability to eliminate the dispersion of calculated values caused by a locally concentrated stress. Fig.11 demonstrates the model with three bridges as an example. The magnet was aligned with the vector potential contour lines and placed in one layer with an electric opening angle of approximately θ_{opt}. The bottom edge of the beam is completely restrained, and summing up the magnet mass M_m and the mass of the upper portion of the magnet M_i, the total mass $M = M_m+M_i$ is arranged to be pulled by the centrifugal force of the rotor around point A, the center of mass M. The width and length of the beam are defined as “a” and “b”, respectively.

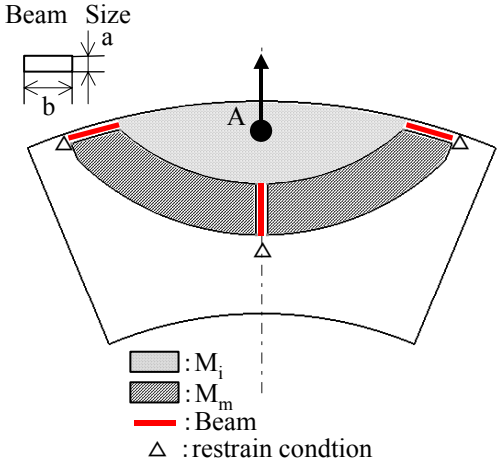

Fig. 11. An example of bridge design model.

Fig.12 shows the maximum stress variation for changing the number of bridges from 2 to 5 under a certain fixed value of beam width "a" and length "b". The target line in the diagram indicates the passable stress predicted on the basis of consideration of the stress requirements that would be determined by manufacturing process and other final stage issues. It can be seen from Fig.12 that three or more bridges mitigate much of the stress.

The torque index variation for different number of bridges under the same stator construction appears in Table.2. The utilization ratio means the ratio of the fundamental components of the magnet flux linkages φ_m which can be obtained by using two kinds of bridge materials; one with iron and other all with air instead. When the bridges are fully composed of air, the value of φ_m decreases as the number of bridges increases. This is because the surface area of magnet is limited by the bridges. The leakage flux of magnet also increases as the number of bridges increases, resulting in the poor utilization ratio of φ_m. On the other hand, there is hardly any change in the q-axis inductance, but the d-axis inductance becomes large being proportional to the number of bridges, so that the inductance difference

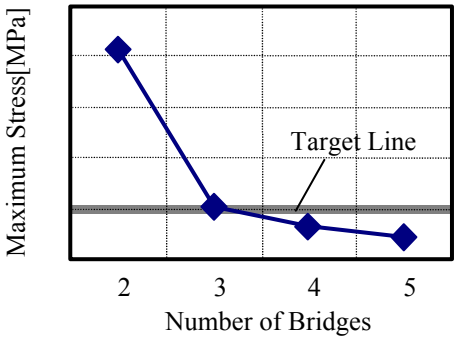

Fig. 12. Bridge quantity and stress.

Table 2. Torque index for number of bridges.

Number of bridges		2	3	4	5
φ_m [Wb]	iron	0.167	0.152	0.138	0.123
	air	0.174	0.166	0.158	0.150
	Utilization Ratio (iron/air)	96%	92%	87%	82%
Inductance [mH]	L_d	0.781	0.864	0.947	1.029
	L_q	2.237	2.237	2.237	2.237
	L_q-L_d	1.456	1.373	1.291	1.208

Table 3. Torque index for bridge of 3,and 2'.

Number of bridges		3	2'
φ_m [Wb]	iron	0.152	0.150
	air	0.166	0.174
	Utilization Ratio (iron/air)	92%	86%
Inductance [mH]	L_d	0.864	1.067
	L_q	2.237	2.261
	L_q-L_d	1.373	1.194

L_q–L_d is degraded.

Take in case of that the number of bridges is set to 2and the bridge width "a" is extended until the stress reaches at the desired value Table 3 summarizes the resulting torque index as 2' compared to that for 3 bridges. It can be found that the flux barrier design using 3 bridges appears to best achieve the rotor mechanical strength while minimizing performance degradation.

4-3. Detailed design

In the actual final design, it is necessary to consider various factors such as material constraints (e.g. magnet demagnetization and mechanical strength of electromagnetic steels), the manufacturing and assembling process issues (e.g. the press equipment used and the minimum shaft diameter and cost

In Fig. 13, the motor developed for the 2000 Prius is compared to our final model meeting for all requirements. The final design has been refined, so that two flat-shape magnets are arranged in a V-shape, and the rotor surface is dimpled to further reduce the iron loss and to minimize torque ripple. In addition to these design refinements, new

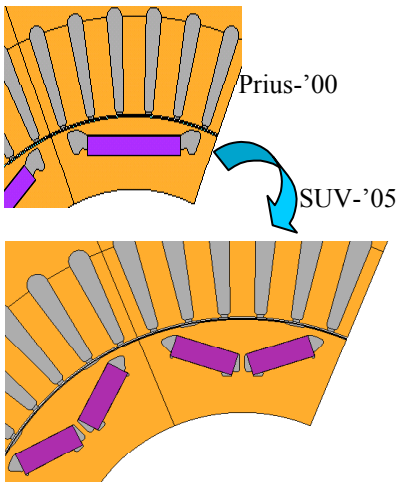

Fig. 13. Final model.

thin electromagnetic steel with low conductivity is applied to the motor developed for THSII in SUV'05. Some optimizations have been also made with regard to welding and press irregularities that aggravate iron loss.

5. Experimental evaluation results of developed motor

Fig.14 shows the speed vs. torque and power characteristics of the newly developed motor for SUV'05. . In the figure, the calculated and measured values are plotted. Both the power and torque reach at levels satisfying the specified requirements of Table 1. In the following section, the motor newly developed is compared against the one developed in 2000 for the Prius.

5-1. Torque characteristics

Fig.15 is a comparison of the torque/weight ratio vs. current phase angle curves under the condition that ampere turn and weight are the same. Despite going down the magnet torque in the newly developed motor by approximately 95% at current phase angle 0 deg., the total maximum torque around at 52 deg. can be approximately 5% improved through an increase in reluctance torque. Although the decrease in the magnet torque at 0 deg is due to the large impact of increasing the number of bridges from 2 to 3 in order to increase the rotor mechanical strength, it contributes to the iron loss reduction under the light-load condition as well as the no-load back-emf limitation.

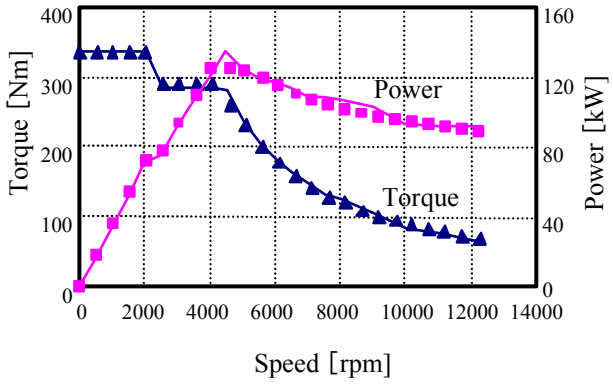

Fig. 14. Power / torque characteristics of newly developed motor.

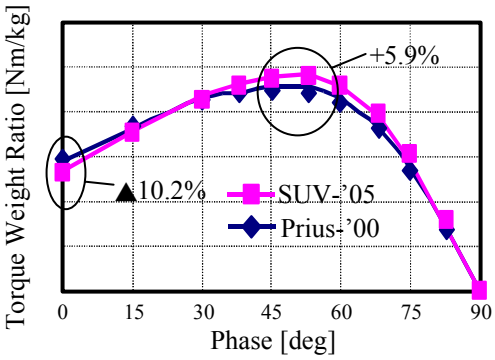

Fig. 15. Torque phase characteristics.

Fig.16 shows the ratio of magnet torque to reluctance torque at each motor under the maximum torque condition. The reluctance torque ratio is significantly increased from 53% to 63%, fulfilling the design objectives.

5-2. Reduction of light-load loss

Fig.17 is a comparison of no-load loss per unit of weight. Under the same speed, an improvement in loss per unit of weight is achieved of over 30%. Of this figure approximately 10% is believed due to improvement in reluctance torque and reduction of harmonics of air-gap flux density distribution, approximately 20% is attributed to employing the high grade electromagnetic steel, and approximately 5% is due to other design refinements.

Figs.18 and 19 illustrate the efficiency map for the 2000 Prius motor and SUV'05 motor respectively. The SUV'05 motor realizes of efficiency above 95% over the most of

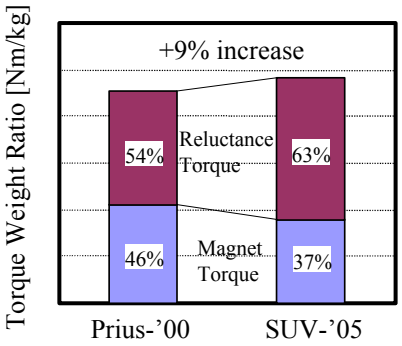

Fig. 16. Torque ratio comparison.

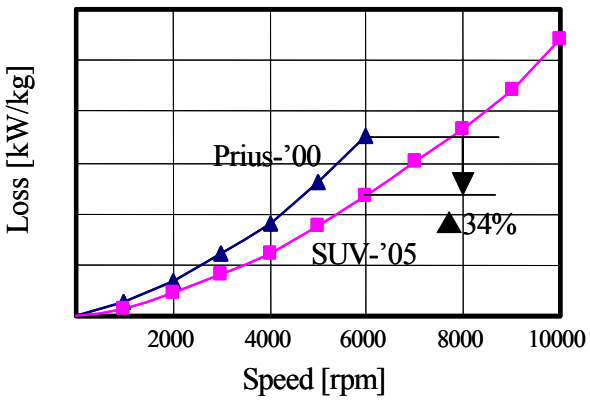

Fig. 17. Measured no-load loss.

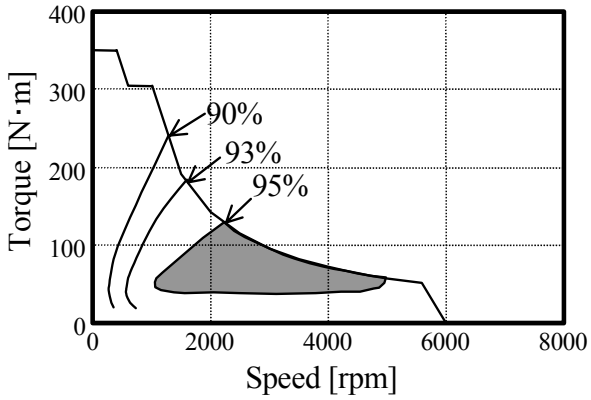

Fig. 18. 2000 Prius motor loss map

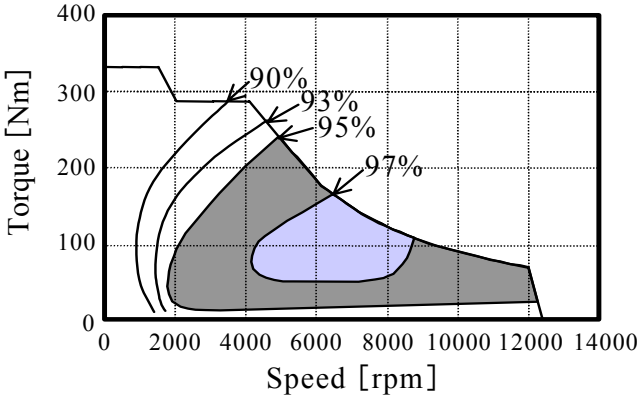

Fig. 19. 2005 SUV motor loss map

operating region, in particular it can be seen to extend to light-load region.

6. Conclusions

The main points of this paper have been able to be summarized as follows.

- In the THS II used in the SUV, a significantly improvement in power weight ratio was carried out by raising motor drive voltage from 500V to 650V, and raising maximum speed to more than double that of previous versions.
- Successful design and developments of the traction drive motor have been achieved, in particular, 1) improvement of rotor strength, 2) reduction of iron loss, and 3) improvement of reluctance torque.
- Placement of magnets along the vector potential contour lines and the use of 3 bridges in rotor construction have proved effective in fulfilling the abovementioned 3 requirements.
- Consequently, we have developed a motor fulfilling the power characteristics requirements, with improved torque density, and over 30% reduced no-load loss.

Traction drive motors such as those for hybrid vehicles will be critical technology for the future. In this paper we have presented remarkable improvements in power weight ratio. However, further developments of electric power trains will be indispensable and hence, we are challenging to progress in downsizing, weight reduction, heightened performance and lowered cost.

Acknowledgement

Thanks are due to President Nobuyuki Matsui and Asst. Prof. Takashi Kosaka, Nagoya Institute of Technology, who provided much encouragement and valuable assistance in preparing this paper.

References

(1) Shinichi Abe : ”Development of the Hybrid Vehicle and its Future Expectation”, SAE 2000-01-C042

(2) M. Okamura, E. Sato, S. Sasaki, ”Development of Hybrid Electric Drive System Using a Boost Converter”, Evs-20, Nov.2003

(3) M. Kamiya, K. Kubo, “Trends in fuel consumption improvement technology for hybrids”. Dengakuron D, Vol. 120, Issue 11, 2000.

(4) T. J. E. Miller, Alan Hutton, Calum Cossar, David A. Staton, “Desingn of a Synchronous Reluctance Motor Drive” , IEEE Trans. on Industry Applications, Vol. 27,No. 4, JULY/AUGUST 1991

(5) M. Kondo, K. Kondo, Y. Fujishima, S. Shinji, “Rotor Design of Permanent Magnet Synchronous Motor for Railway Vehicle”, IEEJ Trans. IA, Vol.124, No.1, 2004

(6) Y. Honda, S. Kawano, H. Kiriyama, .T. higaki, S. Morimoto, Y. Takeda, “Rotor Design and Performances of a Multi-Flux Barrier Synchronous Reluctance Motor “, T. IEEJ. Vol. 118-D, No.10, ’98, p1177- p1184.